Simultaneous Uptake of DMS and Ozone on Water

M. Gershenzon and P. Davidovits*

Department of Chemistry, Merkert Chemistry Center, Boston College, Chestnut Hill, Massachusetts 02467-3809

J. T. Jayne, C. E. Kolb, and D. R. Worsnop

Center for Aerosol and Cloud Chemistry, Aerodyne Research Inc., Billerica, Massachusetts 01821-3976

Received: February 22, 2001; In Final Form: May 7, 2001

The simultaneous uptake of gas-phase DMS−O_3 mixtures by water as a function of temperature (274−300 K) was studied in a bubble train flow reactor. The uptake data yielded the second-order rate constant for the aqueous-phase reaction DMS + O_3 → DMSO + O_2. The reaction products were established with NMR analysis. The reaction rate constant k_2 was measured at four temperatures: 274, 283, 293, and 300 K, yielding $(5.1 \pm 2.0) \times 10^8$ M^{-1} s^{-1}, $(5.9 \pm 2.0) \times 10^8$ M^{-1} s^{-1}, $(8.6 \pm 3.6) \times 10^8$ M^{-1} s^{-1}, and $(11 \pm 4.5) \times 10^8$ M^{-1} s^{-1} respectively. It is noteworthy that the magnitude of the aqueous reaction rate constant exceeds the corresponding gas-phase rate by a factor of about 10^6. The atmospheric importance of the aqueous-phase DMS/O_3 reaction is discussed.

Introduction

Biogenic reduced sulfur compounds, including dimethyl sulfide (DMS, CH_3SCH_3), hydrogen sulfide (H_2S), carbon disulfide (CS_2), methyl mercaptan (CH_3SH), and carbonyl sulfide (OCS), are a major source of sulfur in the marine atmosphere. Their sum is estimated to contribute 15% to 25% of global sulfur emissions.[1−3] These species and their oxidation products, dimethyl sulfoxide (DMSO), dimethyl sulfone ($DMSO_2$), sulfuric and methane sulfonic acids (MSA), dominate production and growth of aerosol and cloud condensation nuclei in the clean marine atmosphere.

Of the biogenically produced species, DMS is the most abundant. Its reactive removal from the atmosphere may occur via gas-phase and liquid-phase reactions within clouds and fog droplets. Its gas-phase oxidative chemistry has been studied extensively. In the gas phase, DMS is oxidized primarily by OH radicals during the day and by NO_3 radicals at night, to produce mainly SO_2, SO_3, MSA (CH_3SO_3H), DMSO ($(CH_3)_2SO$), and $DMSO_2$ ($(CH_3)_2SO_2$).[4−7] The gas-phase reaction of DMS with O_3 was studied by Martinez and Herron.[8] The reaction was found to be slow ($k_{2(gas)} \leq 5 \times 10^2$ M^{-1} s^{-1}), and hence, not significant in the atmosphere.

Gas phase reactions alone do not seem to account fully for the DMS oxidation rate. Current atmospheric models fail to agree with field observations. Recent modeling of field measurements,[9] which considers only gas-phase DMS oxidation pathways, underestimates measured abundance of DMS oxidation products in the marine boundary layer (MBL). Consideration of halogen atom and halogen oxide initiated DMS oxidation cannot resolve the model shortfall. The recommended gas-phase DMS−OH reaction rate constant[10] (2.6×10^9 M^{-1} s^{-1}) would have to be increased by a factor of 3.3 to attain agreement between modeling and field measurements. Another field data/model comparison[11] underpredicts the observed DMSO levels by nearly a factor of 50. These and other studies[12,13] strongly suggest that heterogeneous reactions of DMS may have to be included in the models.

While the gas-phase DMS/O_3 reaction is too slow to be atmospherically significant, recent measurements[14] indicate that the DMS/O_3 heterogeneous aqueous reaction in cloud droplets may be fast enough to contribute to the overall oxidation rate of DMS. The process begins with the uptake of gas-phase DMS and O_3, followed by the liquid-phase reaction of the two solvated species:

$$DMS_{(aq)} + O_{3(aq)} \rightarrow DMSO_{(aq)} + O_{2(aq)} \qquad (R1)$$

In the experiments of Lee and Zhou[14] a DMS/O_3 gas mixture, entrained in an air flow, was bubbled through water. Steady-state DMS and O_3 gas concentrations were reached, and the gas-phase DMS density was monitored as a function of ozone initial concentration. With the Henry's law constants for the two species known, the depletion rate of gas-phase DMS can be determined, and the reaction rate constant computed. The restrictions of such steady-state experiments confine the reagent densities to a narrow range, limiting the accuracy of the measurements. In the Lee and Zhou experiments, the O_3 density was varied from 5×10^{11} to 1.3×10^{12} cm^{-3} and the DMS density from 4.5×10^{10} to 1.2×10^{11} cm^{-3}, a factor of about 2.5 in both cases.

Their experiments were conducted at three temperatures, 278, 288, and 298 K, yielding second-order reaction rate constants of 1.9×10^8, 3.3×10^8, and 6.1×10^8 M^{-1} s^{-1}, respectively, with an accuracy of ±40%. This temperature dependence was expressed in the form of the Arrhenius formulation $k = \nu \cdot \exp(\Delta S/R) \cdot \exp(-\Delta H/RT)$, with an apparent activation energy $\Delta H = 9.6$ kcal/mol and entropy change $\Delta S = 72$ cal·mol^{-1}·K^{-1}, which produces a preexponential factor $A = 5.4 \times 10^{15}$ M^{-1} s^{-1}.

Two aspects of these results seem surprising. First, the DMS/O_3 aqueous reaction rate is very rapid, with the magnitude of the rate constant close to the diffusion-limited rate. Such fast reaction is not typical for other aqueous-phase nonionic sulfur−ozone reactions. For example, methionine, methionine sulfone, and methionine sulfoxide react with ozone with rate constants[15]

10.1021/jp010696y CCC: $20.00
Published on Web 06/20/2001

4×10^6, 1.5×10^5, and 6.6×10^4 M^{-1} s^{-1} respectively. The aqueous O_3/SO_2 reaction has a rate constant of 2.4×10^4 M^{-1} s^{-1} (Hoffmann[16]), and the DMSO/O_3 reaction rate constant is on the order of 10 M^{-1} s^{-1}.[14,15] In a nonpolar solvent, such as carbon tetrachloride, reaction rate constants are somewhat lower:[17] $k_{DMS/O3} = 1.5 \times 10^3$ M^{-1} s^{-1}, $k_{dibutyl\ sulfide/O3} = 1.9 \times 10^3$ M^{-1} s^{-1}, $k_{DMSO/O3} = 7.6$ M^{-1} s^{-1}.

Second, the DMS/O_3 aqueous reaction is at least a factor of 10^6 faster than the corresponding gas-phase reaction. Such dramatic enhancement of the reaction rate constant in the aqueous medium is not expected in general, and is not observed, for example, in a similar hydrogen sulfide reaction with ozone at 293 K: $k_{2(gas)}$ for (H_2S/O_3) is 2.4×10^5 M^{-1} s^{-1} in the gas phase[18] and is 3×10^4 M^{-1} s^{-1} in water.[19]

We also note that in the usual interpretation of the Arrhenius formulation of the rate constant, the preexponential factor A is interpreted as the maximum value of the unhindered rate constant. For reactions in solution, this is the diffusion-limited rate, which is of the order 10^{10} M^{-1} s^{-1} (Benson et al.[20]). The magnitude of the preexponential factor A obtained by Lee and Zhou is a factor of 10^5 higher.

Because of the potential atmospheric importance of the aqueous DMS/O_3 reaction, we decided to address these issues. A series of DMS/O_3 uptake experiments were performed using a recently developed horizontal bubble train flow reactor, modified for co-deposition studies. By contrast with the Lee and Zhou apparatus, here the measurements were not performed under steady-state conditions and the reagent densities can be varied over a significantly wider range. In our experiments, O_3 density was varied by a factor of 6 and the DMS density by a factor of 20.

Experimental Method

The horizontal bubble train apparatus, designed to quantify gas/liquid-phase heterogeneous kinetics, has been described in detail in our previous publications.[21,22] Features pertinent to co-deposition studies are highlighted here. In DMS/O_3 experiments, water is pumped through the 0.4 cm i.d. quartz tube at a controlled speed of about 20−25 cm/sec. A low pressure (50 Torr) gas flow containing the two trace gases of interest (DMS and O_3) diluted in helium carrier gas is injected into the liquid flow via 1.6 mm stainless steel tubing. The two species react in the gas phase; so to minimize gas-phase interaction time, the trace gases are delivered through a coaxial injector in separate helium flows. The two flows merge 10 cm upstream of the injection point. Upon injection into the liquid, the gas forms well-defined bubbles of premixed reagents.

An experimental run begins with the injector positioned outside the flow tube, with the gas flowing through the injector without contacting the liquid, and this "noncontact" signal is recorded. The computer-controlled translation stage then starts to draw the injector into the flow tube filled with the flowing liquid. Well-defined bubbles, filling the diameter of the tube, are formed as the injector enters the liquid. The size, speed, and frequency of the bubbles are monitored by light-emitting diodes positioned 20 cm from the exit of the flow tube. The liquid flow carries the bubbles to the end of the flow tube, where the bubbles open and release the entrained gases for continuous detection by the mass spectrometer, in which the ions are produced by electron impact ionization (70 eV). The contribution of DMS fragment ion peak at $m/z = 48$ to the ozone signal was measured to be less than 3% at all densities used in these experiments. Depending on the experimental run, the densities of the trace gases in the bubble ranged from 5×10^{15} to 3×10^{16} cm^{-3} for O_3 and from 1×10^{15} to 2×10^{16} cm^{-3} for DMS.

Ozone was prepared by passing dry oxygen through a Welsbach T-23 discharge ozonator and stored in a glass trap on silica gel at 195 K. The trap was then connected to the apparatus through a three-way valve, allowing the flow tube to be bypassed in order to pump out adsorbed oxygen. Ozone was entrained in a calibrated flow of helium and its absolute density was determined by absorption of 254 nm mercury light upstream of the injector. Ozone concentration was calculated from Beer's law using absorption cross-section[23] $\sigma_n = 1.15 \times 10^{-17}$ cm^{-2} at 254 nm. Measurements confirmed that no appreciable loss of ozone occurs in the injector.

The DMS/helium mixture was prepared by diluting anhydrous DMS vapor with helium at a DMS/He ratio in the range 0.005−0.03. The mixture was stored in a Teflon coated stainless steel cylinder. The DMS and DMSO used in these experiments were obtained from Aldrich Chemical Co., Inc., (anhydrous 99%+, and 99.9%, respectively). Helium was obtained from AGA Gas Inc., (99.999%). All chemicals were used without further purification. Millipore Milli-Q filtered water (resistivity > 18 MΩ·cm at 25 °C) was used in all of the studies.

Modeling Gas−Liquid Interactions

In general, gas uptake by a liquid is governed by gas-phase diffusion, mass accommodation, and often by solubility constraints as the species in the liquid approach Henry's law saturation. In the latter process, some of the molecules that previously entered the liquid evaporate back into the gas phase due to limited solubility. At equilibrium, the liquid is saturated and the flux of molecules into the liquid becomes equal to the rate of desorption of these molecules out of the liquid, resulting in zero net uptake. Chemical reactions of the solvated species in the bulk liquid or at the gas/liquid interface provide a sink for the species, counteracting the effect of saturation.

General solutions to the uptake equations, which include the effect of gas-phase diffusion, interfacial mass accommodation, Henry's law solubility, chemical reaction in the aqueous bulk phase, and interactions at the gas−liquid interface, are not available. However, in some specific cases, the mass transfer equation can be readily solved (see, for example, Danckwerts[24] and Sherwood and Pigford[25]). A discussion of these treatments is found in Shi et al.[26]

Modeling of gas uptake in the bubble train apparatus begins with the expression for the flux, J, of gas molecules into a semi-infinite liquid in the presence of an irreversible liquid phase chemical reaction. Because the bubble train apparatus is used to measure relatively small uptake probabilities, gas-phase diffusion and mass accommodation do not limit the uptake rate and their effect on uptake is negligible. In the absence of barriers due to these two processes, Danckwerts[24] gives the following expression for the uptake flux due to irreversible reaction in the bulk liquid:

$$J = n_g HRT \cdot [(D_l/\pi t)^{1/2} \exp(-kt) + (D_l k)^{1/2} erf(kt)^{1/2}] \quad (1)$$

Here, n_g is the gas-phase density of the trace species, R is the gas constant (0.082 $dm^3 \cdot atm \cdot K^{-1} \cdot mol^{-1}$), D_l is the diffusion coefficient of the trace species in the liquid, k is the first-order reaction rate constant, T is the temperature, t is the gas−liquid interaction time, and H is the Henry's law coefficient in units $M \cdot atm^{-1}$.

In the limit as $k \rightarrow 0$, eq 1, averaged from $t = 0$ to $t = t'$, yields

$$J(t') = 2 n_g HRT \cdot (D_l/\pi t')^{1/2} \quad (2)$$

As is evident, the flux tends toward zero as the gas−liquid contact time (t') increases, and the liquid approaches saturation. In this case, if D_l is known, the Henry's law coefficient can be obtained from the uptake flux.

In the presence of a fast irreversible chemical reaction of the trace species in the liquid, kt is large and the uptake flux approaches a steady-state value given by

$$J(k) = n_g HRT\cdot(D_l k)^{1/2} \tag{3}$$

In this case, the product $Hk^{1/2}$ can be obtained from uptake measurements. In the intermediate regime, where k is neither negligible nor very large, both H and the product $Hk^{1/2}$ affect the uptake.

The expression for the gas uptake flux in eq 1 is applicable to the uptake of a single gas species. Solution to the mass transfer equations for the case of simultaneous uptake of two gases (gas A and gas B), which react in the liquid phase, cannot be obtained analytically due to nonlinearity of the governing differential equations. Even if the initial condition $[B]_s \gg [A]_s$ were satisfied, a traditional first-order approximation would not apply because of differences in diffusion rates and Henry's law coefficients of the two species. As a result of these differences, the time and distance dependence of the concentrations of species A and B within the liquid are not the same. A number of approximation techniques[27−29] yield results that conform closely to the numerical (exact) solution of this problem. In this work, the approximation of Hikita and Ishikawa[28] has been used. It follows that, in case of the second-order reaction, flux of one component (A) into the liquid can be approximated (to within 10%) by replacing the pseudo-first-order reaction constant k in eq 1 with

$$k = \eta\cdot k_2\cdot[B]_s \tag{4}$$

where k_2 is the second-order rate constant for the aqueous reaction in $M^{-1}\ s^{-1}$, $[B]_s$ is the aqueous concentration in mol/L of the second compound (B) at the interface given by $[B]_s = n_{g(B)}\cdot H_B RT$ ($n_{g(B)}$ is the gas-phase concentration of gas (B), H_B is its Henry's law constant), and η is a coefficient obtained via solution of a transcendental equation

$$\frac{1-\dfrac{1}{q\sqrt{r}}}{3-3\eta^2-\dfrac{1}{q\sqrt{r}}} = \sqrt{\pi}/4\left(\tau\eta+\frac{1}{\tau\eta}\right)\cdot erf(\tau\eta) + 1/2\exp(-\tau^2\eta^2) \tag{5}$$

In this equation, r is the diffusivity ratio $r = D_{l(B)}/D_{l(A)}$; q is the interfacial concentration ratio $q = (n_{g(B)}H_{(B)})/(n_{g(A)}H_{(A)})$, and $\tau = (k_2 n_{g(B)}H_{(B)}RT\cdot t)^{1/2}$ is a dimensionless time parameter.

A self-consistent value for the flux of the second component (B), accounting for the effects of reaction and diffusion, can be then calculated from the flux of (A), provided q is constant with times, as follows:

$$J_B = \frac{1}{q\sqrt{r}}J_A + n_{g(B)}\cdot H_{(B)}RT\cdot\sqrt{\frac{D_{l(B)}}{\pi t}}\cdot\frac{q\sqrt{r}-1}{q\sqrt{r}} \tag{6}$$

In this treatment, the species designation A and B must be chosen so that the product $qr^{1/2}$ is greater than unity.

In the appropriate limits, the expressions for J_A and J_B approach the analytical solution of Danckwerts (eq 1). Thus, when one reagent is in significant excess (i.e., $qr^{1/2} \rightarrow \infty$), coefficient $\eta \rightarrow 1$ and flux J_A is determined by a pseudo-first-order reaction (for times $t \gg 1/\pi k_2[B]_s$), whereas the flux of J_B is governed principally by physical adsorption. If species A and B are identical, as in the case of NO_2 uptake governed by self-reaction,[22] then $qr^{1/2} = 1$, and $\eta \rightarrow \sqrt{2/3}$. Then J_A and J_B are equal and the above formulation is identical to the one given by Cheung et al.[22]

Equations 4 to 6 are the foundation for modeling gas uptake in the horizontal bubble train reactor. Numerical techniques are used to couple the gas density in the bubble to liquid diffusion and reaction processes. The details of the model are presented in Swartz et al.[21] The model takes into account the changing size, shape, and velocity of the bubbles along their path. Model parameters were determined, and the performance of the apparatus was validated by studying the uptake of five reactive systems and eight different species with known Henry's law coefficients. As currently configured, the apparatus can determine $Hk^{1/2}$ values in the range 0.04−150 $M\cdot atm^{-1}\cdot s^{-1/2}$.

Results

Henry's Law Constants. Both DMS and O_3 are individually nonreactive in water. The uptake flux is therefore governed by eq 2, and a measurement of this flux yields a value for the product $HD_l^{1/2}$. The Henry's law and liquid water diffusion coefficients have been previously measured for both DMS and O_3 (H_{O3} by Kosak-Channing,[30] and H_{DMS} by De Bruyn et al.;[31] $D_{l(DMS)}$ by Saltzman et al.,[32] and $D_{l(O3)}$ by Johnson and Davis[33]). However, in these DMS/O_3 studies we first measured the uptake of the two species separately, to obtain independent determinations of the product $HD_l^{1/2}$, which also are required to analyze the reactive uptake flux (see eq 3). Uptake studies yielded $HD_l^{1/2}$ values in the temperature range 274−300 K. From these measurements, using $D_{l(DMS)} = 1.1 \times 10^{-2}\exp(-1896/T(K))$ $cm^2\cdot s^{-1}$ (Salzman et al.[32]) and $D_{l(O3)} = 2.0 \times 10^{-2}\exp(-2178/T(K))$ $cm^2\cdot s^{-1}$ (Johnson and Davis[33]), the following Henry's law coefficients were calculated for DMS and ozone respectively:

$$H_{DMS}\ (M\cdot atm^{-1}) = (4.80 \pm 0.38) \times 10^{-1}\cdot\exp[(3730 \pm 240)\cdot(1/T - 1/T_0)]$$

$$H_{O3}\ (M\cdot atm^{-1}) = (1.07 \pm 0.09) \times 10^{-2}\exp[(2330 \pm 340)\cdot(1/T - 1/T_0)]$$

where $T_0 = 298$ K. These values are within 10% of the previous determinations over the temperature range studied.[30,31]

DMS/O_3 Reaction Rate Constant. The rate constant for the aqueous-phase DMS + O_3 reaction was obtained by measuring the uptake of gas-phase DMS and O_3 as a function of gas-phase species densities. The studies were carried out with O_3 and DMS densities in the range $[O_3] = 5 \times 10^{15}$ to 3×10^{16} cm^{-3} and $[DMS] = 1 \times 10^{15}$ to 2×10^{16} cm^{-3} over the temperature range 274 to 300 K.

Typical simultaneous uptake data at $T = 293$ K are shown in Figure 1 for DMS and O_3 densities of 1.5×10^{16} cm^{-3} and 7×10^{15} cm^{-3}, respectively. Here, the normalized density of the gas-phase species is plotted as a function of the square root of the gas−liquid interaction time. The solid line is the best model fit to the measured DMS/O_3 uptake with rate constant k_2 as the variable parameter. A series of k_2 values are obtained from this fitting procedure. Nonreactive uptake for the two species is displayed as dashed lines.

We note that the characteristic time for the uptake of the gas-phase species into the liquid-phase species is on the order of a

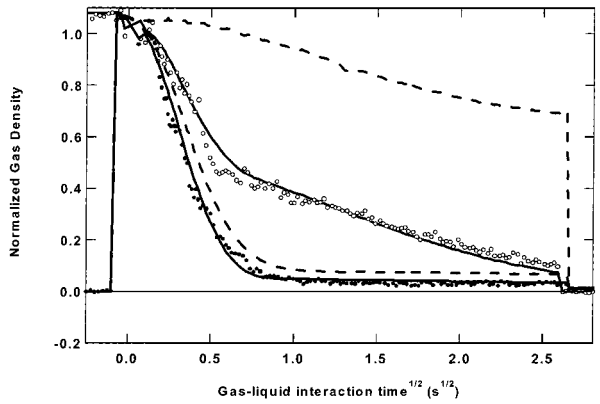

Figure 1. Uptake of DMS (filled circles) and O_3 (open circles) at $[DMS] = 1.5 \times 10^{16}$ cm^{-3} and $[O_3] = 7 \times 10^{15}$ cm^{-3} and $T = 293$ K. Dashed lines represent nonreactive uptake of DMS and ozone.

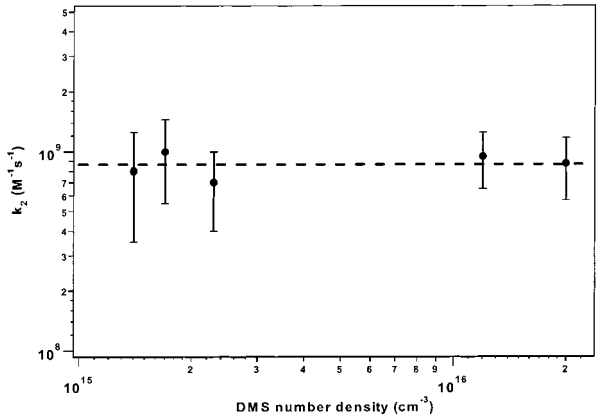

Figure 2. Second-order DMS/O_3 rate constant at $T = 293$ K as a function of DMS concentration. Ozone concentration is in the range $(0.5-3) \times 10^{16}$ cm^{-3}.

second. On the other hand, the characteristic time of DMS/O_3 gas-phase reaction under our experimental conditions is calculated to be greater than 50 s. Therefore, the effect of gas-phase reaction on species decay can be neglected.

The solubility of DMS is significantly higher than that of ozone (at 293 K, $H_{O3} = 1.2 \times 10^{-2}$ M·atm^{-1}; $H_{DMS} = 0.6$ M·atm^{-1}). Therefore, the uptake of DMS is governed mainly by solubility and is more rapid than that of O_3. Its uptake rate is only slightly increased by the presence of O_3. On the other hand, the enhancement of O_3 uptake due to aqueous-phase reaction with DMS is clearly evident. The rate of reactive uptake of ozone is determined by the liquid-phase DMS concentration near the surface. As is evident in the uptake curve in Figure 1, ozone uptake proceeds in two stages. In the initial stage (for times less than about 0.3 s), both O_3 and DMS are simultaneously entering the liquid, diffusing, and reacting within it. Relatively high DMS concentration at the surface is maintained by the DMS influx from the gas phase. At longer interaction times, bulk liquid-phase DMS concentration approaches Henry's law equilibrium. Part of the DMS has reacted in the liquid surface layer, and the rest is diffusively diluted within the bulk. The rate of reactive uptake of O_3 is decreased, reflecting established gas−liquid partitioning of DMS. In this region, DMS concentration is relatively low and ozone uptake is mainly governed by solubility. As is evident, this change in the uptake process is well modeled. In Figure 2 we show values of k_2 as a function of DMS gas-phase density for $T = 293$ K. The reaction is clearly first order with respect to DMS.

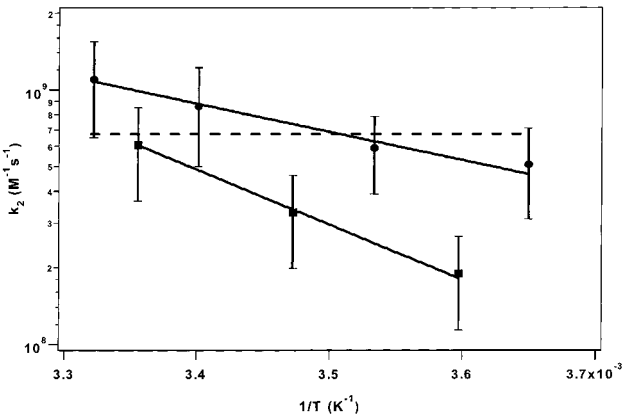

Figure 3. Temperature dependence of the second-order rate constant of DMS/O_3 reaction. Squares represent data reproduced from Lee and Zhou,[14] circles represent data obtained in this study. Solid lines represent best fits to the data in form of Arrhenius equation.

The reaction rate constant k_2 was measured at four temperatures: 274, 283, 293, and 300 K, yielding $(5.1 \pm 2.0) \times 10^8$, $(5.9 \pm 2.0) \times 10^8$, $(8.6 \pm 3.6) \times 10^8$, and $(11 \pm 4.5) \times 10^8$ M^{-1} s^{-1}, respectively. The uncertainty in the quoted k_2 values is the statistical uncertainty representing one standard deviation from the average.

In Figure 3 we plot k_2 on a logarithmic scale as a function of $1/T$. The data of Lee and Zhou[14] are also shown. The error bars for their data points are shown as ±40%, reflecting their stated accuracy. Both data sets show an increase in k_2 with temperature and are well fit by straight lines in the log k vs $1/T$ plot. The rate constant can therefore be expressed in an Arrhenius formulation as k_2(M^{-1} s^{-1}) = $(5.3 \pm 5) \times 10^{12}$·exp(−(2600 ± 280)/$T$). Here, as in the Arrhenius formulation of Lee and Zhou, the preexponential A factor is larger than diffusion-limited rate constant. However, we note that the best-fit Arrhenius formulation quoted above is obtained by a fit to the experimental points and does not take into account the error bars. In fact, within experimental error, k_2 may be temperature independent at a value $k_{2(aq)} = 6.7 \times 10^8$ M^{-1} s^{-1} as shown by the broken line in the figure.

The DMS/O_3 reaction kinetics rate was also studied at $T = 293$ K at pH = 6.8 (unbuffered water) and at pH = 1.0 and 13.7 as maintained by HCl and NaOH. The pH of the samples was determined before and after ozonation reaction with a glass electrode calibrated with standard buffers (pH = 4−10). The observed reaction kinetics for pH = 1 and pH = 13.7 were identical to that in unbuffered solution. We therefore conclude that neither acid nor base catalysis of the reaction is taking place.

Products Analysis. Products of the reaction (R1) were confirmed in a set of independent experiments using NMR spectroscopy. Here, ozone was bubbled through a 20 mM solution of DMS in deuterated water for approximately 20 min. The solution was continuously stirred. Samples were collected every 5 min and analyzed later with an NMR spectrometer. The gradual decrease of the DMS signal was accompanied by a simultaneous appearance and growth of peaks corresponding to DMSO and $DMSO_2$. No other reaction products were detected. At the end point, conversion of DMS to DMSO and $DMSO_2$ is close to unity.

Role of the DMSO−O_3 Reaction. DMSO(aq) is a product of the DMS + O_3 reaction. While previous experiments[14,15] indicated that the aqueous reaction of O_3 with the product DMSO molecule is too slow to contribute significantly to O_3 decay kinetics, we decided to confirm this in the present study. The uptake of gas-phase O_3 by DMSO aqueous solutions

TABLE 1: Principal DMS Oxidation Processes in the Atmosphere[a]

	DMS				
	Second-order rate constant k_2, ($M^{-1}s^{-1}$)		Atmospheric lifetime τ		
reactant	$T = 273$ K	$T = 298$ K	$T = 273$ K	$T = 298$ K	ref
$OH_{(g)}$	2.4×10^9	2.6×10^9	2.9 days	2.7 days	10
$NO_{3(g)}$	7.6×10^8	6.5×10^8	0.4 days	0.4 days	10
$O_{3(g)}$		<603		>17 days	10
$OH_{(in-cloud)}$		1.9×10^{10}		97 days	40
$NO_{3(in-cloud)}$		$\sim 2 \times 10^{10}$		~8200 days	diffusion-limited,20
$O_{3(in-cloud)}$	1.2×10^8	6.1×10^8	17.5 days	18.8 days	14
$O_{3(in-cloud)}$	**3.9×10^8**	**8.6×10^8**	5.4 days	13.4 days	this work

[a] The following values were used in the calculations: Fractional liquid water content $L = 3 \times 10^{-7}$, daily average concentrations of oxidants $[OH] = 1 \times 10^6$ cm^{-3} (Krol et al.[41]), $[NO_3] = 2.5 \times 10^7$ cm^{-3} (Allan et al.[42]), $[O_3] = 6.5 \times 10^{11}$ cm^{-3} (Logan et al.[43]). Henry's law coefficients: at 298 K; $H_{OH} = 40$ M·atm^{-1} (Hanson et al.[44]); $H_{NO3} = 0.018$ M·atm^{-1} (Poskrebyshev et al.[45]); $H_{O3} = 1.1 \times 10^{-2}$ M·atm^{-1} (this work), $H_{DMS} = 0.48$ M·atm^{-1} (this work). At 273 K: $H_{O3} = 2.1 \times 10^{-2}$ M·atm^{-1} (this work), $H_{DMS} = 1.5$ M·atm^{-1} (this work).

(concentration 0.02 to 4.5 M) was measured with the bubble-train apparatus. Our measured value for the DMSO/O_3 rate constant is $k'_{2(aq)} = 4.3 \pm 1$ M^{-1} s^{-1}, at 293 K, consistent with the previously measured values of 5.7 M^{-1} s^{-1} (Lee and Zhou[14]) and 8.2 M^{-1} s^{-1} (Pryor et al.[15]).

Discussion

The results of these experiments confirm that the DMS/O_3 reaction rate is indeed very rapid, as observed by Lee and Zhou.[14] On the other hand, the temperature dependence of the reaction rate constant measured in our studies is smaller than that quoted by Lee and Zhou. In their experiments, the rate constant increases from 1.9×10^8 to 6.1×10^8 M^{-1} s^{-1} as the temperature increases from 278 to 298 K. In our experiments, over a similar temperature range, the rate constant increases from $(5.1 \pm 2.0) \times 10^8$ to $(11 \pm 4.5) \times 10^8$ M^{-1} s^{-1}. We note that in their published figure of k_2 vs. $1/T$, Lee and Zhou showed error bars of about ±10%. However, in the text they report an accuracy of ±40% at 288 K. If one applies larger (±40%) error bars to the data of Lee and Zhou (as in Figure 3), the two sets of measurements are brought to a near agreement within the larger error limits.

We now suggest a possible explanation for the high DMS/O_3 aqueous reaction rate (10^6 times higher than in the gas phase). In the gas phase, the reaction is thought to proceed through a cyclic intermediate, resulting from electrophilic addition of the ozone molecule to the sulfur and one of the methyl groups.[8] This is followed by scission of O−O and C−S bonds. Thus, in the gas phase, the major products of DMS/O_3 oxidation are H_2CO, H_2O, CO, and SO_2.[8] Direct conversion of DMS to DMSO is not observed in the gas phase.

In solution, C−S bond scission does not occur. The conversion of DMS to sulfoxide and sulfone is complete. The reaction rate constant[17] in CCl_4 is 10^5 times lower than the one measured in water. This suggests that the solvent plays a key role in the fate of the DMS−O_3 adduct. It is most likely that the cyclic intermediate is not formed in solution, rather the reaction proceeds via the polar adduct as shown. A polar solvent such

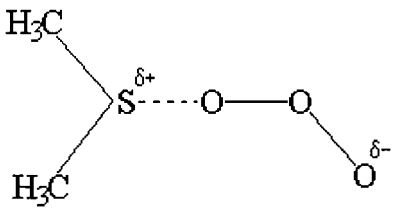

as water would stabilize the adduct and facilitate its conversion to DMSO. Alternatively, as proposed by Razumovskii et al.,[17] the reaction may proceed through a cationic chain mechanism that will be likewise accelerated in a polar solvent. Quantum chemical calculations are in progress to explore the role of the solvent in this reaction.

Atmospheric Implications. The fractional liquid water content (L) of tropospheric clouds is typically 3×10^{-7} cm^3/cm^3. In-cloud aqueous reactions compete with analogous gas-phase reactions when the species are highly soluble or their reaction rates are significantly enhanced in the aqueous medium. Expanding the methodology of Noziere et al.,[34] the gas and aqueous phase reaction rates for two species A and B, under conditions of gas−liquid equilibrium, are equal when

$$(RT)^2 H_A H_B L[A][B] k_{2(aq)} = [A][B] k_{2(g)} \qquad (8)$$

Here [A] and [B] are gas-phase concentrations (mole/L) of species A and B, H_A and H_B are their Henry's law constants, $k_{2(g)}$ and $k_{2(aq)}$ are gas and aqueous phase reaction rate constants in M^{-1} s^{-1}, and R is the gas constant, 0.082 dm^3·atm·K^{-1}·mol^{-1}. At $T = 298$ K and L $= 3 \times 10^{-7}$ cm^3/cm^3, we obtain

$$H_A H_B (k_{2(aq)}/k_{2(g)}) = 5300 \text{ (M·atm}^{-1})^2 \qquad (9)$$

Equation 9 shows that for species of low solubility, with Henry's law constants on the order of 0.1 M·atm^{-1}, aqueous reactions become significant when $k_{(aq)} > 5 \times 10^5 \, k_{(gas)}$. For many compounds gas-phase and aqueous-phase reaction rates do not differ by more than one or two orders of magnitude. (See for example Atkinson,[35] Mallard et al.,[36] Razumovskii,[37] Ross et al.[38]) The DMS/O_3 reaction is clearly an exception. Here $k_{2(aq)} \geq 10^6 \, k_{2(g)}$, and with the cited H values, the ratio $H_A H_B (k_{2(aq)}/k_{2(g)})$ in eq 9 is greater than 6000. Therefore, we expect the oxidation rate of DMS by O_3 in clouds to be faster than in the gas phase.

In Table 1 we compare characteristic reaction time of DMS/O_3 in-cloud reaction to other DMS oxidative removal processes in the gas and aqueous phases. This is an expanded version of the data found in Lee and Zhou[14] and in Finlayson-Pitts and Pitts.[39] The principal oxidants considered are OH, NO_3, and O_3. The atmospheric lifetimes (τ) are calculated as inverse pseudo-first-order rate constants. The values of the parameters used in calculating τ are listed in the footnote to the table. Of course, not all marine air is cloud or fog filled, so accurate comparison of DMS loss rates would require a fully interactive and representative coupled atmospheric chemistry/meteorology model with accurate cloud dynamics.

As shown in the table, the present study predicts a shorter DMS lifetime with respect to heterogeneous O_3 reaction than predicted by the work of Lee and Zhou. However, both results

substantiate the conclusion that the in-cloud oxidation rate of DMS by ozone can be appreciable as compared to gas-phase reactions with OH and NO_3 radicals. Further, the sources and sinks of the radicals are such that OH reaction occurs during daytime, oxidation by NO_3 takes place principally at night, and in-cloud O_3 oxidation occurs during both periods.

The contribution of the DMS/O_3 in-cloud oxidation channel depends on temperature via the parameters H and k_2, which have opposite temperature dependencies. As is evident, the importance of the DMS/O_3 in-cloud oxidation channel increases as the temperature decreases, due to the dominance of negative temperature dependence of Henry's law constants. Because of the steeper positive temperature dependence of k_2 reported by Lee and Zhou, the overall temperature effect of in-cloud oxidation is more pronounced in our results (see Table 1). In either case, it is evident that in-cloud oxidation of DMS by O_3 should be included in atmospheric models, particularly for remote marine air where NO_3 radical concentrations may be quite low.

Acknowledgment. Funding for this work was provided by the National Science Foundation Grants No. ATM-99-05551 and CH-0089147, by the Department of Energy Grant No. DE-FG02-98ER62581, by the U.S.−Israel Binational Science Foundation Grant No. 1999134.

References and Notes

(1) Penner, J. E.; Atherton, C. A.; Graedel, T. E. *Global atmospheric-biospheric chemistry*; Prinn, R., Ed.; Plenum Press: New York, 1994; 223−248.

(2) Lelieveld, J.; Roelofs, G.-J.; Ganzeveld, L.; Feichter, J.; Rodhe, H. *Philos. Trans. R. Soc. London B* **1997**, *352*, 149−158.

(3) Watts, S. F. *Atmos. Environ.* **2000**, *34*, 761−779.

(4) Yin, F.; Grosjean, D.; Seinfeld, J. H. *J. Atmos. Chem.* **1990**, *11*, 309−364.

(5) Lin, X.; Chameides, W. L. *Geophys. Res. Lett.* **1993**, *20*, 579−582.

(6) Lovejoy, E. R.; Ravishankara, A. R.; Howard, C. J. *Int. J. Chem. Kinet.* **1994**, *26*, 552−560.

(7) Stickel, R. E.; Chin, M.; Daykin, E. P.; Hynes, A. J.; Wine, P. H.; Wallington, T. J. *J. Phys. Chem.* **1993**, *97*, 13, 653−13, 661.

(8) Martinez, R. I.; Herron, J. T. *Int. J. Chem. Kinet.* **1978**, *10*, 433−452.

(9) James, J. D.; Harrison, R. M.; Savage, N. H.; Allen, A. G.; Grenfell, J. L.; Allan, B. J.; Plane, J. M. C.; Hewitt, C. N.; Davison, B.; Robertson, L. *J. Geophys. Res.* **2000**, *105*, 26379−26392.

(10) Atkinson, R.; Baulch, D. L.; Cox, R. A.; Hampson, R. F.; Kerr, J. A.; Rossi, M. J.; Troe, J. *J. Phys. Chem. Ref. Data* **1997**, *26*, 1329−1499.

(11) Chen, G.; Davis, D. D.; Kasibhatla, P.; Bandy, A. R.; Thornton, D. C.; Huebert, B. J.; Clarke, A. D.; Blomquist, B. W. *J. Atmos. Chem.* **2000**, *37*, 137−160.

(12) Campolongo, F.; Saltelli, A.; Jensen, N. R.; Wilson, J.; Hjorth, J. *J. Atmos. Chem.* **1999**, *32*, 327−356.

(13) Davis, D.; Chen, G.; Bandy, A.; Thornton, D.; Eisele, F.; Mauldin, L.; Tanner, D.; Lenschow, D.; Fuelberg, H.; Huebert, B.; Heath, J.; Clarke, A.; Blake, D. *J. Geophys. Res.−Atmos.* **1999**, *104*, 5765−5784.

(14) Lee, Y.; Zhou, X. *J. Geophys. Res.* **1994**, *99*, 3597−3605.

(15) Pryor, W. A.; Giamalva, D. H.; Church, D. F. *J. Am. Chem. Soc.* **1984**, *106*, 7094−7100.

(16) Hoffmann, M. R. *Atmos. Environ.* **1986**, *20*, 1145−1154.

(17) Razumovskii, S. D.; Shatokhina, E. I.; Malievskii, A. D.; Zaikov, G. E. *Bull. Acad. Sci. USSR D. Chem. Sci.* **1975**, *24*, 469−472.

(18) Glavas, S.; Toby, S. *J. Phys. Chem.* **1975**, *79*, 779−782.

(19) Hoigne, J.; Bader, H.; Haag, W. R.; Staehelin, J. *Water Res.* **1985**, *19*, 993−1004.

(20) Benson, S. W. *The foundations of chemical kinetics*; McGraw-Hill: New York, 1960; Chapter XV.

(21) Swartz, E.; Boniface, J.; Tchertkov, I.; Rattigan, O.; Robinson, D. V.; Davidovits, P.; Worsnop, D. R.; Jayne, J. T.; Kolb, C. E. *Environ. Sci. Technol.* **1997**, *31*, 2634−2641.

(22) Cheung J. L.; Li, Y. Q.; Boniface, J.; Shi, Q.; Davidovits, P.; Worsnop, D. R.; Jayne, J. T.; Kolb, C. E. *J. Phys. Chem. A* **2000**, *104*, 2655−2662.

(23) DeMore, W. B.; Sander, S. P.; Golden, D. M.; Hampson, R. F.; Kurylo, M. J.; Howard, C. J.; Ravishankara, A. R.; Kolb, C. E.; Molina, M. J. *Chemical kinetics and photochemical data for use in stratospheric modeling;* Evaluation number 12, NASA, JPL, 1997.

(24) Danckwerts, P. V. *Gas−Liquid Reactions*, McGraw-Hill: New York, 1970; Chapter 3.

(25) Sherwood, T. K.; Pigford, R. L. *Absorption and Extraction*, 2nd ed.; McGraw-Hill: New York, 1952; p 329.

(26) Shi, Q.; Li, Y. Q.; Davidovits, P.; Jayne, J. T.; Worsnop, D. R.; Mozurkewich, M.; Kolb, C. E. *J. Phys. Chem. B* **1999**, *103*, 2417−2430.

(27) Ramachandran, P. A.; Sharma, M. M. *Trans. Inst. Chem. Eng.* **1971**, *49*, 253−280.

(28) Hikita, H.; Ishikawa, H. *Ind. Eng. Chem. Fundam.* **1977**, *16*, 215−219.

(29) Zarzycki, R.; Ledakowicz, S.; Starzak, M. *Chem. Eng. Sci.* **1981**, *36*, 113−121.

(30) Kosak-Channing, L. F.; Helz, G. R. *Environ. Sci. Technol.* **1983**, *17*, 145−149.

(31) De Bruyn, W. J.; Swartz, E.; Hu, J. H.; Shorter, J. A.; Davidovits, P.; Worsnop, D. R.; Zahniser, M. S.; Kolb, C. E. *J. Geophys. Res* **1995**, *100*, 7245−7251.

(32) Saltzman, E. S.; King, D. B.; Holmen, K.; Leck, C. *J. Geophys. Res.−Oceans* **1993**, *98*, 16481−16486.

(33) Johnson, P. N.; Davis, R. A. *J. Chem. Eng. Data* **1996**, *41*, 1485−1487.

(34) Noziere B.; Longfellow, C. A.; Henry, B. E.; Voisin, D.; Hanson, D. R. to be published.

(35) Atkinson, R. *Atmos. Environ.* **1990**, *24*, 1−41.

(36) Mallard, W. G.; Westley, F.; Herron, J. T.; Hampson, R. F.; Frizzell, D. H. *NIST chemical kinetics database, Ver 5.0*, NIST standard reference data: Gaithersburg, MD, 1993.

(37) Razumovskii, S. D. *Russ. Chem. Bull.* **1995**, *44*, 2287−2288.

(38) Ross, A. B.; Mallard, W. G.; Helman, W. P.; Buxton, G. V.; Huie, R. E.; Neta, P. *NDRL-NIST solution kinetics database, Ver. 3*, Notre Dame radiation laboratory: Notre Dame, IN, and NIST standard reference data, Gaithersburg, MD, 1998.

(39) Finlayson-Pitts, B. J.; Pitts, J. N., Jr. *Chemistry of the Upper and Lower Atmosphere*, Academic Press: San Diego, 2000, pp 328−334.

(40) Bonifacic, M.; Moeckel, H.; Bahnemann, D.; Asmus, K. D. *J. Chem. Soc., Perkin Trans.* 2, **1975**, 675−685.

(41) Krol, M.; Van Leeuwen, P. J.; Lelieveld, J. *J. Geophys. Res.−Atmos.* **1998**, *103*, 10697−10711.

(42) Allan, B. J.; McFiggans, G.; Plane, J. M. C.; Coe, H.; McFadyen, G. G. *J. Geophys. Res.−Atmos.* **2000**, *105*, 24191−24204.

(43) Logan, J. A. *J. Geophys. Res−Atmos.* **1999**, *104*, 16115−16149.

(44) Hanson, D. R.; Burkholder, J. B.; Howard, C. J.; Ravishankara, A. R. *J. Phys. Chem.* **1992**, *96*, 4979−4985.

(45) Poskrebyshev, G. A.; Neta, P.; Huie R. E. *J. Geophys. Res.* **2001**, *106*, 4995−5004.